Applied Mathematics Letters 26 (2013) 232–239

Contents lists available at SciVerse ScienceDirect

Applied Mathematics Letters

journal homepage: www.elsevier.com/locate/aml

A GN model for thermoelastic interaction in an unbounded fiber-reinforced anisotropic medium with a circular hole

Ibrahim A. Abbas *

Department of Mathematics, Faculty of Science and Arts - Khulais, King Abdulaziz University, Jeddah, Saudi Arabia
Department of Mathematics, Faculty of Science, Sohag University, Sohag, Egypt

ARTICLE INFO

Article history:
Received 21 June 2012
Received in revised form 1 September 2012
Accepted 1 September 2012

Keywords:
Green and Naghdi theory
Fiber-reinforced
Finite element method

ABSTRACT

In this work, we have constructed the equations for generalized thermoelasticity of an unbounded fiber-reinforced anisotropic medium with a circular hole. The formulation is applied in the context of Green and Naghdi (GN) theory. The thermoelastic interactions are caused by (I) a uniform step in stress applied to the boundary of the hole with zero temperature change and (II) a uniform step in temperature applied to the boundary of the hole which is stress-free. The solutions for displacement, temperature and stresses are obtained with the help of the finite element procedure. The effects of the reinforcement on temperature, stress and displacement are studied. Results obtained in this work can be used for designing various fiber-reinforced anisotropic elements under mechanical or thermal load to meet special engineering requirements.

1. Introduction

During the second half of the twentieth century, non-isothermal problems in the theory of elasticity became increasingly important. This is due to their many applications in widely diverse fields. First, the high velocities of modern aircraft give rise to aerodynamic heating, which produces intense thermal stresses that reduce the strength of the aircraft structure. Second, in the nuclear field, the extremely high temperature and temperature gradients originating inside nuclear reactors influence their design and operations [1]. Materials such as resins reinforced with strong aligned fibers exhibit highly anisotropic elastic behavior in the sense that their elastic moduli for extension in the fiber direction are frequently of the order of 50 or more times greater than their elastic moduli in transverse extension or in shear. The mechanical behavior of many fiber-reinforced composite materials is adequately modeled by the theory of linear elasticity for transversely isotropic materials, with the preferred direction coinciding with the fiber direction. In such composites the fibers are usually arranged in parallel straight lines. However, other configurations are used. An example is that of circumferential reinforcement, for which the fibers are arranged in concentric circles, giving strength and stiffness in the tangential (or hoop) direction. The theory of strongly anisotropic materials has been extensively discussed in the literature. Belfield et al. [2] studied the stress in elastic plates reinforced with fibers lying in concentric circles. Sengupta and Nath [3] discussed the problem of surface waves in fiber-reinforced anisotropic elastic media. Singh [4] showed that, for wave propagation in fiber-reinforced anisotropic media, this decoupling cannot be achieved by the introduction of the displacement potentials. Hashin and Rosen [5] studied the elastic moduli for fiber-reinforced materials. The classical theory of thermoelasticity as exposed for example in Carlson's article [6] has found generalizations and modifications into various thermoelastic models that go under the label hyperbolic thermoelasticity; see the survey of Chandrasekharaiah [7] and Hitnarski and Ignazack [8]. The description "hyperbolic" reflects the fact that thermal waves are modeled, avoiding the physical paradox of infinite propagation speed of the classical

* Correspondence to: Department of Mathematics, Faculty of Science and Arts - Khulais, King Abdulaziz University, Jeddah, Saudi Arabia.
E-mail address: ibrabbas7@yahoo.com.

0893-9659/$ – see front matter © 2012 Elsevier Ltd. All rights reserved.
doi:10.1016/j.aml.2012.09.001

model. In the decade of the 1990's Green and Naghdi [9–11] proposed three new thermoelastic theories based on an entropy equality rather than the usual entropy inequality. Singh [12] studied the wave propagation in thermally conducting linear fiber-reinforced composite materials with one relaxation time. Verma [13] studied the problem of magnetoelastic shear waves in self-reinforced bodies. Chattopadhyay and Choudhury [14] investigated the propagation, reflection and transmission of magnetoelastic shear waves in self-reinforced media. Chattopadhyay and Choudhury [15] discussed the propagation of magnetoelastic shear waves in an infinite self-reinforced plate. Chattopadhyay and Michel [16] gave a model for spherical SH-wave propagation in self-reinforced linearly elastic media. Tian et al. [17], Abbas [18] and Abbas and Abdalla [19] applied the finite element method in different generalized thermoelastic problems.

The exact solution of the governing equations of the generalized thermoelasticity theory for a coupled and nonlinear/linear system exists only for very special and simple initial and boundary problems. To calculate the solution for general problems, a numerical solution technique is used. For this reason the finite element method is chosen. The method of weighted residuals offers the formulation of the finite element equations and yields the best approximate solutions to linear and nonlinear boundary and partial differential equations (see Wriggers [20]).

This work considers a thermoelastic problem involving such circumferentially reinforced plates. The composite material is then locally transversely isotropic, with the direction of the axis of transverse isotropy now not constant, but everywhere directed along the tangents to circles in which the fibers lie. The problem has been solved numerically using a finite element method (FEM). Numerical results for the temperature distribution, the displacement and the stress components are represented graphically.

2. Formulation of the problem

Following [9–12], the basic equations of Green and Naghdi theory, for a fiber-reinforced linearly thermoelastic anisotropic medium whose preferred direction is that of a unit vector $\boldsymbol{a}$, in the absence of body forces and heat sources, are considered as follows:

The equations of motion:

$$\tau_{ij,j} = \rho \ddot{u}_i, \quad i, j = 1, 2, 3. \tag{1}$$

The heat conduction equations:

$$K^* T_{,ii} + K_{ij} \dot{T}_{,ii} = \rho c_e \ddot{T} + T_o \beta_{ij} \ddot{u}_{i,i}, \quad i, j = 1, 2, 3. \tag{2}$$

The constitutive equation (stress–strain and temperature relations) is given by

$$\begin{aligned} \tau_{ij} &= \lambda e_{kk} \delta_{ij} + 2\mu_T e_{ij} + \alpha (a_k a_m e_{km} \delta_{ij} + a_i a_j e_{kk}) + 2(\mu_L - \mu_T)(a_i a_k e_{kj} + a_j a_k e_{ki}) \\ &\quad + \beta\, a_k a_m\, e_{km} a_i a_j - \beta_{ij}\, (T - T_o)\, \delta_{ij}, \quad i, j, k, m = 1, 2, 3, \end{aligned} \tag{3}$$

where T is the temperature change of a material particle; T_o is the reference uniform temperature of the body; ρ is the mass density; the u_i are the displacement vector components; e_{ij} is the strain tensor; τ_{ij} is the stress tensor; β_{ij} is the thermal elastic coupling tensor; K_{ij} is the thermal conductivity; K^* is the material characteristic of the theory; c_e is the specific heat at constant strain; α, β, and $(\mu_L - \mu_T)$ are reinforced anisotropic elastic parameters; λ, μ_T are elastic parameters; and the components of the vector $\boldsymbol{a}$ are (a_1, a_2, a_3) where $a_1^2 + a_2^2 + a_3^2 = 1$. The superimposed dot represents time differentiation and the comma notation is used for spatial derivatives. For circumferential reinforcement the vector $\boldsymbol{a}$ is everywhere directed in the tangential (i.e. θ) direction, so in cylindrical polar coordinates $\boldsymbol{a}$ has components (0, 1, 0). We use a cylindrical system of coordinates (r, θ, z); for this axially symmetric problem we have $u = u(r, t)$, where r is the radial distance measured from the origin (point of symmetry), and the stress tensor is determined by the radial stress τ_{rr} and the circumferential stress (hoop stress) $\tau_{\theta\theta}$. Therefore, the radial strain e_{rr} and the hoop strain $e_{\theta\theta}$ are given by

$$e_{rr} = \frac{\partial u}{\partial r}, \qquad e_{\theta\theta} = \frac{u}{r}. \tag{4}$$

It is assumed that there are no body forces and heat sources in the medium. So, the equation of motion and energy equation have the forms

$$\frac{\partial \tau_{rr}}{\partial r} + \frac{1}{r}(\tau_{rr} - \tau_{\theta\theta}) = \rho \frac{\partial^2 u}{\partial t^2}, \tag{5}$$

$$K^* \left(\frac{\partial^2 T}{\partial r^2} + \frac{1}{r} \frac{\partial T}{\partial r} \right) + \frac{\partial}{\partial t} \left(K_{11} \frac{\partial^2 T}{\partial r^2} + K_{22} \frac{1}{r} \frac{\partial T}{\partial r} \right) = \frac{\partial^2}{\partial t^2} \left(\rho c_e T + T_o \beta_{11} \frac{\partial u}{\partial r} + T_o \beta_{22} \frac{u}{r} \right), \tag{6}$$

$$\tau_{rr} = (\lambda + 2\mu_T) \frac{\partial u}{\partial r} + (\lambda + \alpha) \frac{u}{r} - \beta_{11} (T - T_o), \tag{7}$$

$$\tau_{\theta\theta} = (\lambda + \alpha) \frac{\partial u}{\partial r} + (\lambda + 2\alpha + 4\mu_L - 2\mu_T + \beta) \frac{u}{r} - \beta_{22} (T - T_o), \tag{8}$$

with $\beta_{11} = 2(\lambda + \mu_T)\alpha_{11} + (\lambda + \alpha)\alpha_{22}$, $\beta_{22} = 2(\lambda + \alpha)\alpha_{11} + (\lambda + 2\alpha + 4\mu_L - 2\mu_T + \beta)\alpha_{22}$, where α_{11}, α_{22} are the coefficients of linear thermal expansion. For convenience, the following non-dimensional variables are used:

$$\begin{aligned} &(r', u') = c_1\chi(r, u), \qquad t' = c_1^2\chi t, \qquad \left(\tau'_{rr}, \tau'_{\theta\theta}\right) = \frac{1}{D}\left(\tau_{rr}, \tau_{\theta\theta}\right), \qquad \chi = \frac{\rho c_e}{K_{11}}, \\ &T' = \frac{T - T_o}{T_o}, \qquad c_1 = \sqrt{\frac{D}{\rho}}, \qquad D = \lambda + 2\alpha + 4\mu_L - 2\mu_T + \beta. \end{aligned} \tag{9}$$

In terms of the non-dimensional quantities defined in Eqs. (9), the above governing equations reduce to (dropping the dashes for convenience)

$$\frac{\partial}{\partial r}\left(B_1\frac{\partial u}{\partial r} + B_2\frac{u}{r} - B_3T\right) + (B_1 - B_2)\frac{1}{r}\frac{\partial u}{\partial r} + (B_2 - 1)\frac{u}{r^2} - (B_3 - B_4)\frac{T}{r} = \frac{\partial^2 u}{\partial t^2}, \tag{10}$$

$$\varepsilon_1\left(\frac{\partial^2 T}{\partial r^2} + \frac{1}{r}\frac{\partial T}{\partial r}\right) + \frac{\partial}{\partial t}\left(\frac{\partial^2 T}{\partial r^2} + \varepsilon_2\frac{1}{r}\frac{\partial T}{\partial r}\right) = \frac{\partial^2}{\partial t^2}\left(T + \varepsilon_3\frac{\partial u}{\partial r} + \varepsilon_4\frac{u}{r}\right), \tag{11}$$

$$\tau_{rr} = B_1\frac{\partial u}{\partial r} + B_2\frac{u}{r} - B_3T, \tag{12}$$

$$\tau_{\theta\theta} = B_2\frac{\partial u}{\partial r} + \frac{u}{r} - B_4T, \tag{13}$$

where $(B_1, B_2, B_3, B_4) = \frac{1}{D}(\lambda + 2\mu_T, \lambda + \alpha, T_o\beta_{11}, T_o\beta_{22})$, $(\varepsilon_1, \varepsilon_2, \varepsilon_3, \varepsilon_4) = \left(\frac{K^*}{\rho c_e c_1^2}, \frac{K_{22}}{K_{11}}, \frac{\beta_{11}}{\rho c_e}, \frac{\beta_{22}}{\rho c_e}\right)$.

3. Boundary conditions

We consider boundary conditions of two types:

(I) The surface of the hole, i.e. $r = 1$, is subjected to a step input of radial stress and zero temperature change, so the boundary conditions are taken as

$$\tau_{rr}(1, t) = -\sigma_o H(t), \qquad T(1, t) = 0, \quad t > 0. \tag{14}$$

(II) The surface of the hole, i.e. $r = 1$, is assumed to be stress-free and is subjected to a uniform step in the temperature effect, so the boundary conditions are taken as

$$\tau_{rr}(1, t) = 0, \qquad T(1, t) = T_1H(t), \quad t > 0, \tag{15}$$

where $H(t)$ denotes the Heaviside unit step function. The medium is assumed to be at rest and undisturbed initially. The initial and regularity conditions are

$$u = T = 0 \quad at\ t = 0, \qquad r \geq 1, \qquad \frac{\partial u}{\partial t} = \frac{\partial T}{\partial t} = 0 \quad at\ t = 0 \quad \text{and} \quad u, T \to 0 \text{ when } r \to \infty. \tag{16}$$

4. The finite element method

The finite element method is a powerful technique originally developed for numerical solution of complex problems in structural mechanics, and it remains the method of choice for complex systems. A further benefit of this method is that it allows physical effects to be visualized and quantified regardless of experimental limitations. In this section, the governing equations of generalized thermoelasticity based upon Green and Naghdi theory are summarized, using the corresponding finite element equations. In the finite element method, the displacement component u and temperature T are related to the corresponding nodal values by

$$u = \sum_{i=1}^{m} N_i u_i(t), \qquad T = \sum_{i=1}^{m} N_i T_i(t), \tag{17}$$

where m denotes the number of nodes per element, and N the shape functions. In the framework of the standard Galerkin procedure, the weighting functions and the shape functions coincide. Thus,

$$\delta u = \sum_{i=1}^{m} N_i \delta u_i, \qquad \delta T = \sum_{i=1}^{m} N_i \delta T_i. \tag{18}$$

Table 1
Grid independence test ($t = 0.3$, $r = 1.5$).

Mesh size	Case I		Case II	
	$T \times 10^{-3}$	$u \times 10^{-8}$	$T \times 10^{-1}$	$u \times 10^{-6}$
1,000	8.324960	4.244323	3.538151	1.326896
3,000	8.323887	4.243051	3.538154	1.326914
6,000	8.323808	4.242957	3.538155	1.326915
9,000	8.323790	4.242934	3.538155	1.326916
12,000	8.323788	4.242933	3.538155	1.326916

With Eqs. (17) and (18), $u' = u_{,i}$ and $T' = T_{,i}$ can be expressed as

$$u' = \sum_{i=1}^{m} N_i' u_i(t), \qquad T' = \sum_{i=1}^{m} N_i' T_i(t), \tag{19}$$

$$\delta u' = \sum_{i=1}^{m} N_i' \delta u_i, \qquad \delta T' = \sum_{i=1}^{m} N_i' \delta T_i. \tag{20}$$

Thus, the finite element equations corresponding to Eqs. (10) and (11) can be obtained as

$$\sum_{e=1}^{me} \left(\begin{bmatrix} M_{11}^e & 0 \\ M_{21}^e & M_{22}^e \end{bmatrix} \begin{Bmatrix} \ddot{u}^e \\ \ddot{T}^e \end{Bmatrix} + \begin{bmatrix} 0 & 0 \\ 0 & C_{22}^e \end{bmatrix} \begin{Bmatrix} \dot{u}^e \\ \dot{T}^e \end{Bmatrix} + \begin{bmatrix} K_{11}^e & K_{12}^e \\ 0 & K_{22}^e \end{bmatrix} \begin{Bmatrix} u^e \\ T^e \end{Bmatrix} = \begin{Bmatrix} F_1^e \\ F_2^e \end{Bmatrix} \right), \tag{21}$$

where *me* is the total number of elements. The coefficients in Eq. (21) are presented in the Appendix. Symbolically, the discretized equations of Eqs. (21) can be written as

$$M\ddot{d} + C\dot{d} + Kd = F^{ext}, \tag{22}$$

where M, C, K and F^{ext} represent the mass, damping, stiffness matrices and external force vectors, respectively; $d = [u\ T]^T$; on the other hand, the time derivatives of the unknown variables have to be determined, by the Newmark time integration method (see Wriggers [20]).

5. A numerical example

With a view to illustrating and comparing the theoretical results obtained in the previous sections in the context of the GN model of thermoelasticity, we now present some numerical results. The physical data for the material are given as [12]

$$\rho = 2660\ \text{kg/m}^3, \quad \lambda = 5.65 \times 10^{10}\ \text{N/m}^2, \quad \mu_T = 2.46 \times 10^{10}\ \text{N/m}^2,$$
$$\mu_L = 5.66 \times 10^{10}\ \text{N/m}^2, \quad T_1 = 1, \quad \sigma_o = 1,$$
$$\alpha = -1.28 \times 10^{10}\ \text{N/m}^2, \quad \beta = 220.90 \times 10^{10}\ \text{N/m}^2, \quad \alpha_{11} = 0.017 \times 10^{-4}\ \text{deg}^{-1},$$
$$\alpha_{22} = 0.015 \times 10^{-4}\ \text{deg}^{-1}, \quad t = 0.3,$$
$$c_e = 0.787 \times 10^3\ \text{J kg}^{-1}\,\text{deg}^{-1}, \quad K_{11} = 0.0921 \times 10^3\ \text{J m}^{-1}\text{s}^{-1}\,\text{deg}^{-1},$$
$$K_{22} = 0.0963 \times 10^3\ \text{J m}^{-1}\text{s}^{-1}\,\text{deg}^{-1}, \quad T_o = 293\ \text{k}.$$

Before going to the analysis, the grid independence test has been conducted and the results are presented in Table 1. The grid size has been refined and consequently the values of different parameters as observed from Table 1 are stabilized. Further refinement of mesh size over 12,000 elements does not change the values very considerably, and this is therefore accepted as the grid size for computing purposes.

Using this data set, the displacement u, temperature T, and radial and circumferential stresses τ_{rr}, $\tau_{\theta\theta}$ are numerically computed for different values of the radial distance r and their graphical representation is presented in Figs. 1–8. The solid line (−) refers to thermoelastic solid without reinforcement (NRE) and the dotted line (· · ·) refers to thermoelastic solid with reinforcement (WRE). As expected, the reinforcement has a great effect on the distribution of field quantities.

Case (I): Fig. 1 represents the radial variations of displacement with reinforcement (WRE) and without reinforcement (NRE). It is observed that the displacement is continuous and the displacement gradually decreases with r and is zero at $r = 1.35$ for NRE, and is zero at $r = 1.1$ for WRE. This is also in agreement with the theoretical result where beyond the thermal wave front, displacement vanishes. As shown in Fig. 2, the value of the temperature under NRE increases sharply in the range $1 < r < 1.4$ and then decreases for $r \geq 1.4$ while the value of the temperature under WRE increases sharply in the range $1 < r < 1.1$ and then decreases for $r \geq 1.1$. Fig. 3 shows the graphical presentation of radial stress versus distance r and indicates finite jumps at the elastic wave fronts at $r = 1.45$ for NRE and $r = 1.1$ for WRE. Fig. 4 gives the variation of hoop stress versus r. The hoop stress at first decreases and then suffers a finite jump at the elastic wave front at $r = 1.2$ for

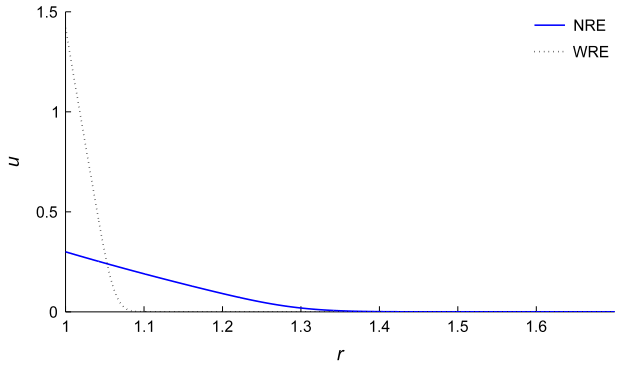

Fig. 1. Case (I): the variations of displacement.

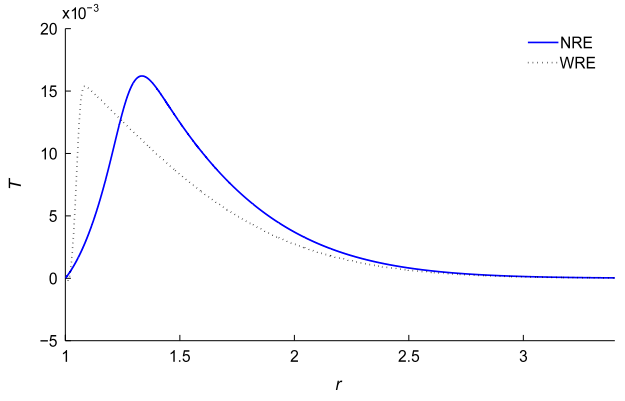

Fig. 2. Case (I): the variations of temperature.

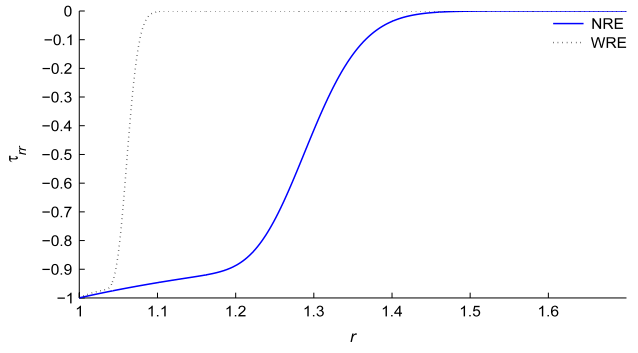

Fig. 3. Case (I): the variations of radial stress.

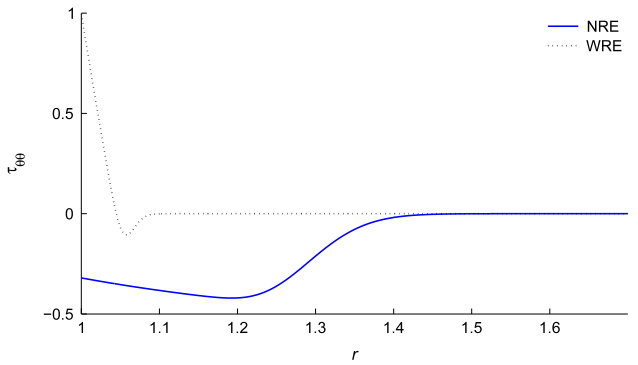

Fig. 4. Case (I): the variations of hoop stress.

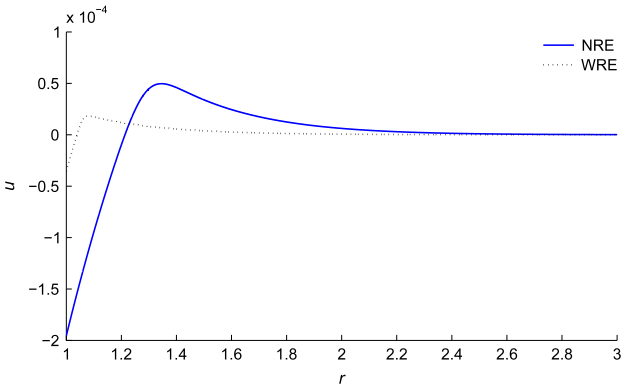

Fig. 5. Case (II): the variations of displacement.

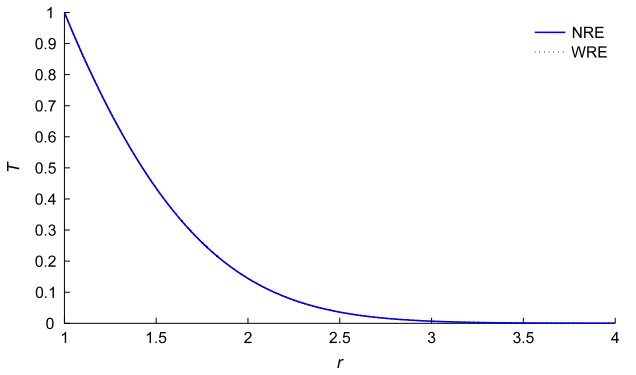

Fig. 6. Case (II): the variations of temperature.

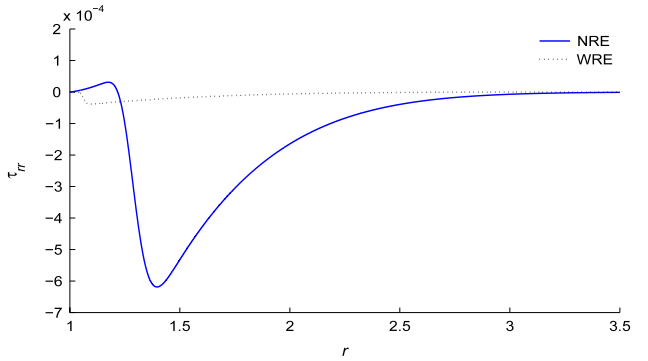

Fig. 7. Case (II): the variations of radial stress.

NRE, and at $r = 1.08$ for WRE, and then it approaches and ultimately becomes zero. This is in agreement with the theoretical result that the disturbance is zero beyond the thermal wave front.

Case (II): The displacement is negative at $r = 1$ where its magnitude is maximum, as in Fig. 5. The displacement increases from the negative value to a positive value. In the positive values, the displacement has a peak value that depends on the presence and absence of reinforcement. Fig. 6 shows that the temperature decreases as r increases. Figs. 7 and 8 depict the variations of radial and hoop stresses with respect to r for the presence and absence of reinforcement; in these we observe that the radial stress is zero at $r = 1$, which satisfies the boundary conditions of the problem, and the reinforcement has a great effect on the distribution of stresses.

6. Conclusion

In this work we have investigated the generalized thermoelastic interaction in an infinite fiber-reinforced anisotropic plate containing a circular hole with Green and Naghdi (GN) theory. The problem has been solved numerically using a finite

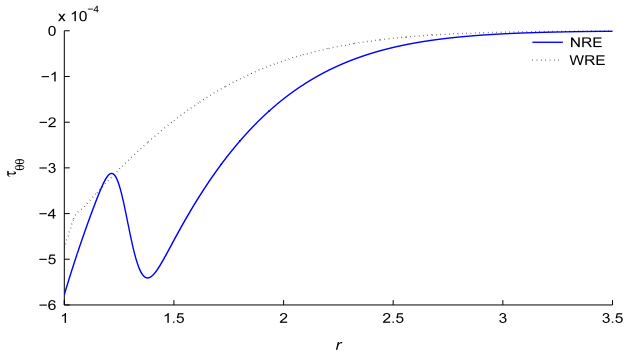

Fig. 8. Case (II): the variations of hoop stress.

element method (FEM). The differences of the field quantities predicted by the GN theory in the presence and absence of reinforcement are remarkable. The reinforcement has a great effect on the distribution of field quantities. The results which are obtained in this work may be used for designing various fiber-reinforced anisotropic thermoelastic elements under mechanical or thermal load to meet special engineering requirements.

Acknowledgments

This work was funded by the Deanship of Scientific Research (DSR), King Abdulaziz University, Jeddah, under Grant No. (7-857-D1432). The authors, therefore, acknowledge with thanks the technical and financial support from DSR.

Appendix

The coefficients that appeared in Eq. (21) are given by

$$M^e_{11} = \int [N]^T [N]\, dr, \qquad M^e_{21} = \int [N]^T \left(\varepsilon_3 [N'] + \frac{\varepsilon_4}{r}[N]\right) dr, \qquad M^e_{22} = \int [N]^T [N]\, dr,$$

$$C^e_{22} = \int \left([N']^T [N'] - \frac{\varepsilon_2}{r}[N]^T [N']\right) dr, \qquad F^e_1 = [N]^T \bar{\tau}\,\big|_1^r, \qquad F^e_2 = [N]^T \bar{q}\,\big|_1^r,$$

$$K^e_{11} = \int \left[[N']^T \left(B_1 [N'] + \frac{B_2}{r}[N]\right) - [N]^T \left(\frac{B_1 - B_2}{r}[N'] + \frac{B_2 - 1}{r^2}[N]\right)\right] dr,$$

$$K^e_{12} = \int \left[-[N']^T B_3 [N] + \frac{B_3 - B_4}{r}[N]^T [N]\right] dr,$$

$$K^e_{22} = \int \left[\varepsilon_1 [N']^T [N'] - \frac{\varepsilon_1}{r}[N]^T [N']\right] dr,$$

where $\bar{\tau}$ represents the component of the traction, and $\bar{q}$ represents the heat flux.

References

[1] J.L. Nowinski, Theory of Thermoelasticity with Applications, Sijthoff & Noordhoof International, Alphen aan den Rijn, 1978.
[2] A.J. Belfield, T.G. Rogers, A.J.M. Spencer, Stress in elastic plates reinforced by fibres lying in concentric circles, J. Mech. Phys. Solids 1 (1983) 25–54.
[3] P.R. Sengupta, S. Nath, Surface waves in fibre-reinforced anisotropic elastic media, Sādhanā 26 (2001) 363–370.
[4] S.J. Singh, Comments on: surface waves in fibre-reinforced anisotropic elastic media, by Sengupta and Nath, Sādhanā 27 (2002) 1–3; Sādhanā 26 (2001) 363–370.
[5] Z. Hashin, W.B. Rosen, The elastic moduli of fibre reinforced materials, J. Appl. Mech. 31 (1964) 223–232.
[6] D.E. Carlson, Linear Thermoelasticity, Vol. 97, Handbuch der Physik. Via/2, 1972, p. 346.
[7] D.S. Chandrasekharaiah, A note on the uniqueness of solution in the linear theory of thermoelasticity without energy dissipation, J. Elast. 43 (1996) 279–283.
[8] R.B. Hetnarski, J. Ignazack, Generalized thermoelasticity, J. Therm. Stresses 22 (1999) 451–476.
[9] A.E. Green, P.M. Naghdi, A re-examination of the basic postulates of thermomechanics, Proc. R. Soc. Lond. A 432 (1991) 171–194.
[10] A.E. Green, P.M. Naghdi, On undamped heat waves in an elastic solid, J. Therm. Stresses 15 (1992) 253–264.
[11] A.E. Green, P.M. Naghdi, Thermoelasticity without energy dissipation, J. Elast. 31 (1993) 189–208.
[12] B. Singh, Wave propagation in thermally conducting linear fibre-reinforced composite materials, Arch. Appl. Mech. 75 (2006) 513–520.
[13] P.D.S. Verma, Magnetoelastic shear waves in self-reinforced bodies, Internat. J. Engrg. Sci. 24 (7) (1986) 1067–1073.
[14] A. Chattopadhyay, S. Choudhury, Propagation, reflection & transmission of magnetoelastic shear waves in a self-reinforced media, Internat. J. Engrg. Sci. 28 (6) (1990) 485–495.
[15] A. Chattopadhyay, S. Choudhury, Magnetoelastic shear waves in an infinite self-reinforced plate, Int. J. Numer. Anal. Methods Geomech. 19 (4) (1995) 289–304.

[16] A. Chattopadhyay, V. Michel, A model for spherical SH-wave propagation in self-reinforced linearly elastic media, Arch. Appl. Mech. 75 (2–3) (2006) 113–124.
[17] X. Tian, Y. Shen, C. Chen, T. He, A direct finite element method study of generalized thermoelastic problems, Int. J. Solids Struct. 43 (2006) 2050–2063.
[18] I.A. Abbas, Finite element analysis of the thermoelastic interactions in an unbounded body with a cavity, Forsch. Ingenieurwes. 71 (2007) 215–222.
[19] I.A. Abbas, A.N. Abd-alla, Effects of thermal relaxations on thermoelastic interactions in an infinite orthotropic elastic medium with a cylindrical cavity, Arch. Appl. Mech. 78 (2008) 283–293.
[20] P. Wriggers, Nonlinear Finite Element Methods, Springer, Berlin, Heidelberg, 2008.